

## **A Sustainable Nitrogen-Doped Functionalized Graphene Nanosheets for Visible-Light-Induced Photocatalytic Water Splitting**

### **EXPERIMENTAL SECTION**

#### **Materials**

All chemicals used in this study were of analytical grade and used as obtained. Urea and methanol were purchased from Sigma Aldrich. Ultrapure water was used throughout the experiments. The pear (*Pyrus pyrifolia*) was purchased from a local supermarket and used as a carbon source without pretreatment.

#### **Synthesis of N-fGNS**

N-fGNS were synthesized using the pear and urea as precursors by the simple hydrothermal method. Typically, 50 g of the peeled and crushed pear was mixed with 5 g of urea using a kitchen mixer and treated hydrothermally in a Teflon-line-coated stainless-steel autoclave for 48 h at 250 °C. After natural cooling to room temperature, the resulting black mass was thoroughly washed with water to remove impurities. Subsequently, the dried sample was pyrolyzed at 900 °C in an inert atmosphere for 1 h at a heating rate of 5 °C min<sup>-1</sup>. The N doping was controlled by altering the amount of urea (1, 3, 5, 8 g). The nitrogen-free f-GNS was synthesized in a similar manner without the addition of urea.

A series of efficient hydrolysis, dehydration, polymerization via condensation and aromatization reactions with subsequent carbonization via intramolecular dehydration of pear results in carbon nano sheets with high oxygenated functional groups.<sup>1, 2</sup> Nitrogen enriched urea act as nitrogen source and plays a key role in the formation of nitrogen-doped graphene nanosheets. During the hydrothermal process decomposition of urea generate NH<sub>3</sub> in a sustained manner, which react with oxygenated functional groups of carbon intermediates and form pyrrolic nitrogen via intramolecular hydrolysis.<sup>3, 4</sup> Simultaneously, some of the NH<sub>3</sub> get protonated and seep into

the carbon skeleton of the biomass along with the time and transferred to graphitic nitrogen or replace the carbon atom in graphitic lattice and resulted in pyridinic nitrogen.<sup>3-5</sup> Further these species reorganize through a series of reactions results in nitrogen-doped graphene nano sheets.<sup>5</sup> Large numbers of surface defects and functional groups were introduced during the hydrothermal carbonization under mild conditions. However, the appropriate mechanism for the conversion of biomass into graphene is still not well understood and needs further exploration. Carbonization at 900 °C under an inert atmosphere was then carried out to produce N-fGNS. The nitrogen content of N-fGNS could be controlled by regulating the concentration of urea during the hydrothermal synthesis indicating the high controllability of this approach.

### **Material characterizations**

The morphology and microstructure of N-fGNS were determined by TEM and HRTEM using a FEI Tecnai G2 F30 microscope operated at 300 kV. The crystallinity and phase structure of the synthesized N-fGNS were characterized by XRD (Rigaku RINT-2000). The elemental composition and chemical states were analyzed by XPS (ULVAC-PHI X electron system) with Al  $K_{\alpha}$  radiation. EuroEA Elemental Analyser was used to analyze the chemical composition of N-fGNS. The functional groups of N-fGNS were analyzed by FTIR spectrometry (BRUKER Vector22, Germany) in a solid state. The optical properties were studied by UV-visible DRS (PerkinElmer, UK) using BaSO<sub>4</sub> as the internal reflectance standard. Room-temperature steady-state PL spectra were recorded using a Varian fluorescence spectrometer in the solid state. The PL spectra were acquired in a solid state by excitation with a 400 nm light irradiation at room temperature. Time-resolved PL spectra were recorded using EasyLife II fluorometer system at an excitation wavelength of 400 nm. The Raman spectrum was acquired with a WITec Raman spectrometer at a laser excitation wavelength of 405 nm. Thermogravimetric analysis (TGA) was conducted to analyze the thermal stability of N-fGNS using a Mettler thermal analyzer under argon atmosphere at 10 °C min<sup>-1</sup> heating rate. Microstructure of N-fGNS was measured with Field-emission scanning electron microscopy (FESEM) using a SUPRA 40VP (Carl Zeiss NTS GmbH, Germany) microscope at an 10kV of accelerating voltage. A Pico SPM (Molecular Imaging) atomic force microscope was used to analyze topology and thickness of N-fGNS.

### **Electrochemical measurements**

All electrochemical measurements were carried out on an Autolab PGSTAT204 potentiostat in a typical two electrode system with aqueous electrolyte (0.1 M KOH). The as-synthesized N-fGNS was thoroughly mix with conductive acetylene black and polytetrafluoroethylene in 8:1:1 ratio and rolled to a 30  $\mu\text{m}$  thin sheet. The obtained sheet was applied evenly on to a 1  $\text{cm}^2$  surface of nickel foam. The transient photocurrents measurements were performed when the electrodes were irradiated with a 150 W halogen lamp at a distance of 10 cm.

### **Photocatalytic water splitting**

The water splitting was carried out in a purely photocatalytic system, which can be operated in a continuous manner with the use of common materials. The photocatalytic water splitting was carried out in a Pyrex round-bottom flask, degassed using  $\text{N}_2$  for 30 min to remove the remnant air. N-fGNS was introduced in a closed flask containing degassed water with 30% of methanol as a sacrificial agent. The photocatalytic water splitting experiments were performed under the visible light irradiation of the 60-W tungsten lamp set at a distance of 25 cm. The temperature was controlled by a water bath to avoid the heating effect by the visible light illumination. The rates of evolved gases were monitored at 30 min by a gas chromatograph (Agilent 490 Micro GC with a thermal conductivity detector and argon as a carrier).

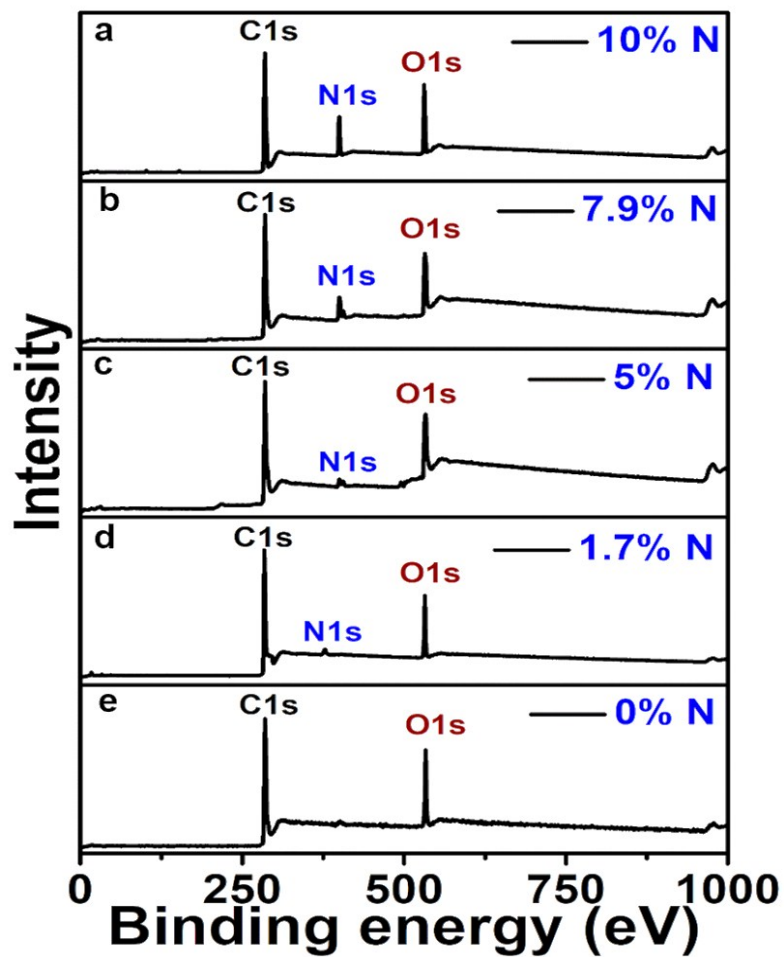


**Fig. S1** Survey scan XPS spectra of N-fGNS clearly showing the controlled doping of nitrogen with (a) 10 %N; (b) 7.9 %N; (c) 5 %N; (d) 1.7 %N; (e) control f-GNS synthesized without the use of urea.

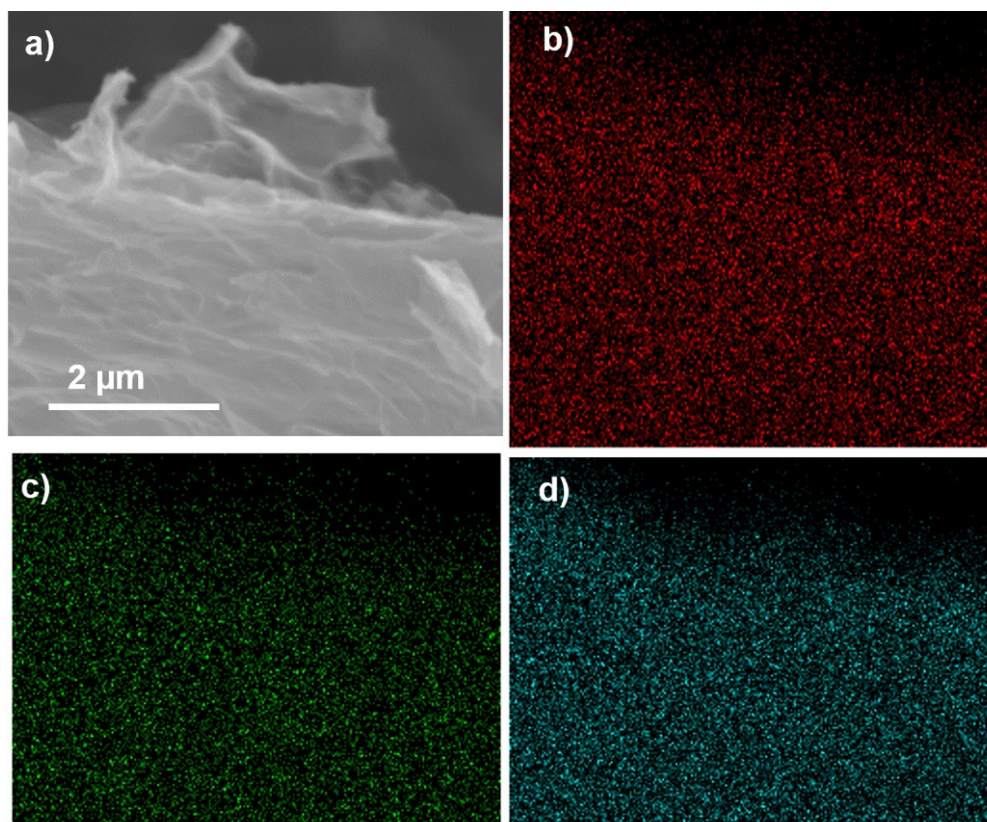


**Fig. S2** (a) SEM image and corresponding elemental mapping of N-fGNS (b) C, (c) O and (d) N.

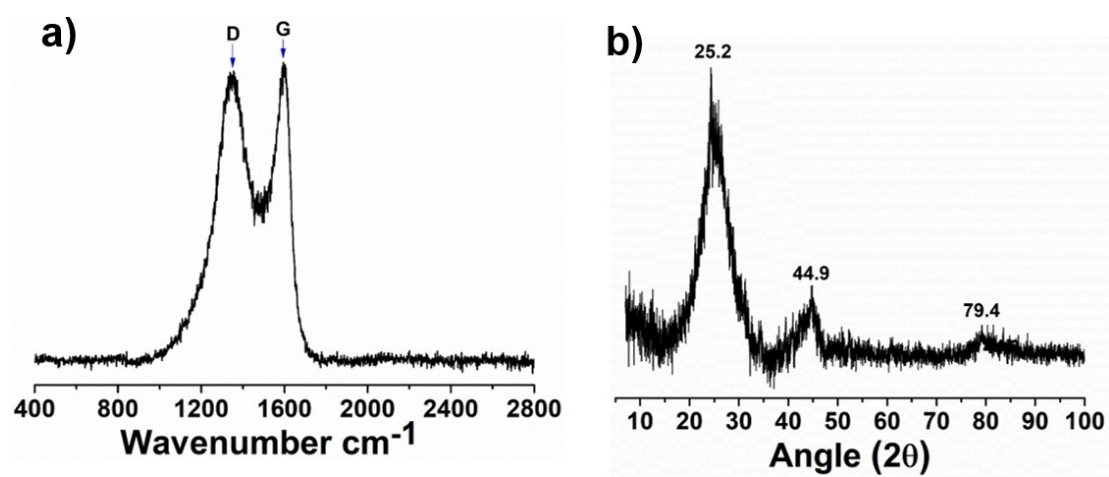


**Fig. S3** Structural characteristics of N-fGNS. (a) Raman spectrum, and (b) XRD pattern revealing the graphitic structure of N-fGNS.

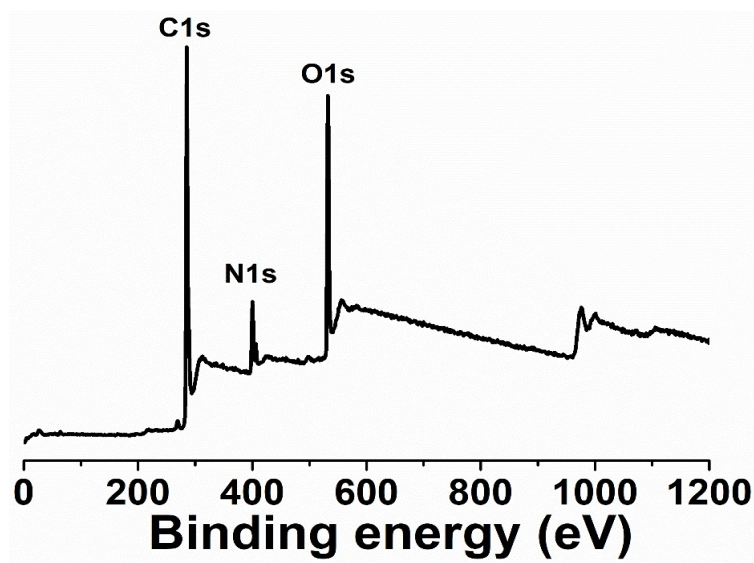


**Fig. S4** Survey scan XPS spectra of N-fGNS clearly showing the presence of only C, O and N elements.

### Optical characterization

The average radiative lifetime ( $A\tau$ ) of the charge carriers of samples follows the orders N-fGNS (7.9% N) > N-fGNS (5% N) > N-fGNS (10% N) > N-fGNS (1.7% N) > fGNS (0% N), suggesting the density of N-doping has significant influence on the lifetime of charge carriers. N-fGNS exhibits  $A\tau$  of 11.58 ns (5% N), 9.62 ns (10% N), 5.62 ns (1.7% N) and 4.99 ns (0% N).

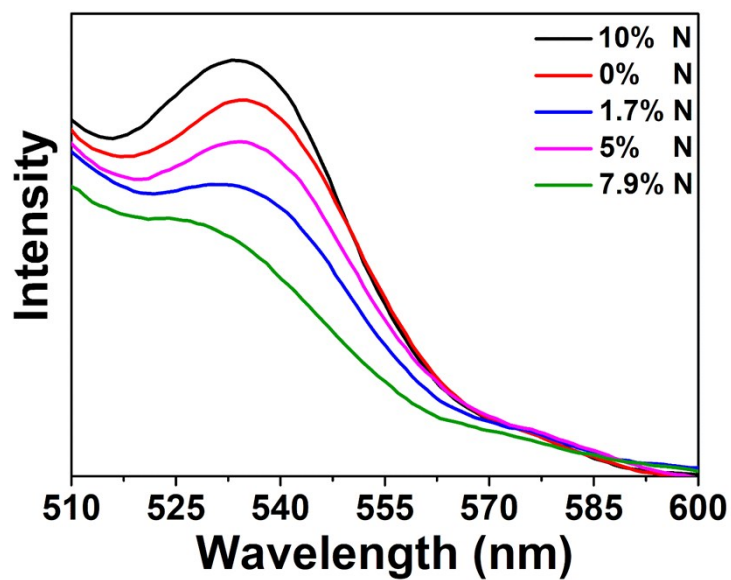


**Fig. S5** Photoluminescence (PL) spectra of the N-fGNS samples with different nitrogen contents.

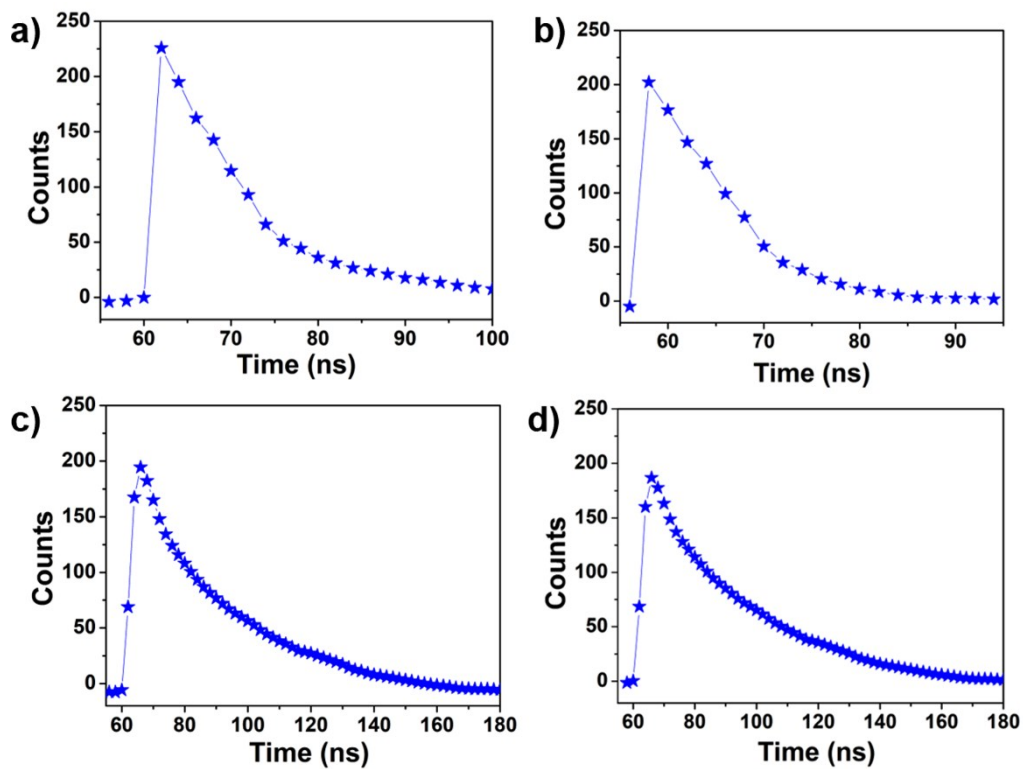


**Fig. S6** Time-resolved PL spectra acquired at an excitation wavelength of 400 nm. (a) N-fGNS with 5% N; (b) N-fGNS with 10% N; (c) N-fGNS with 1.7% N; (d) fGNS.



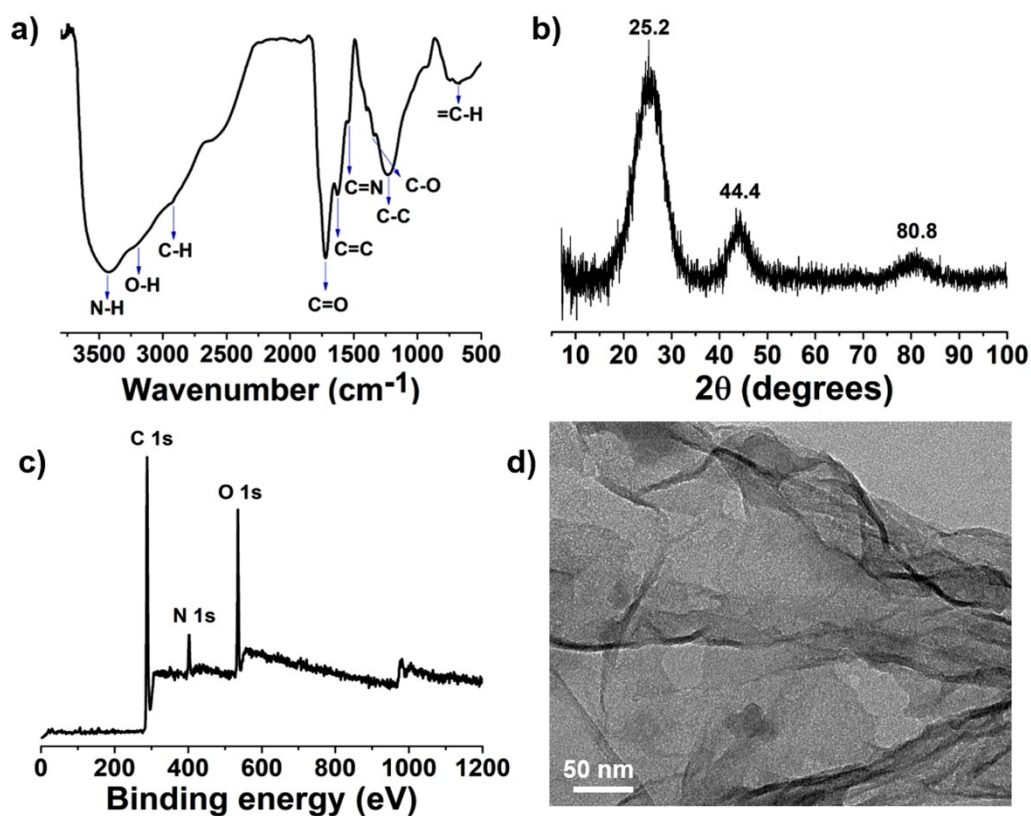


**Fig. S7 Structural and morphological characterizations of N-fGNS after 10 repetitive photocatalytic water splitting cycles. (a)** FTIR spectrum showing no change in structural integrity. **(b)** Raman spectrum showing the phase purity. **(c)** Full-range XP spectrum. **(d)** TEM image showing wrinkled graphene layers.



**Table S1.** Composition of N-fGNS (determined from the electron microprobe)

Element	Atomic%
C K	76.63
O K	15.25
N K	8.13

**Table S2.** Composition of N-fGNS (determined from the full-range XPS spectrum) synthesized with varied amount of urea.

Amount of urea used	% of C	% of N	% of O
0 g	85.75	0	14.24
1 g	85.85	1.7	12.48
3 g	69.81	5	25.02
5 g	76.62	7.9	15.49
7 g	69.13	10	20.87

**Table S3.** Summary of graphene-based photocatalytic materials for water splitting activity

Catalysts	Co-catalyst	Light Source	H <sub>2</sub> evolution rate ( $\mu\text{mol g}^{-1} \text{h}^{-1}$ )	O <sub>2</sub> evolution rate ( $\mu\text{mol g}^{-1} \text{h}^{-1}$ )	Ref.
N-fGNS	None	60 W Tungsten lamp	1380	689	This work
[Ru-dpbpy] /SrTiO <sub>3</sub> :Rh (4 at%)- rGO/BiVO <sub>4</sub>	None	300 W xenon lamp, $\lambda \geq 420 \text{ nm}$	~175	~87.5	6
CuFeO <sub>2</sub> -rGO (H <sub>2</sub> evolution-catalyst)  Bi <sub>20</sub> TiO <sub>32</sub> -rGO(O <sub>2</sub> evolution-catalyst)	Pt/Ru	500-W Hg-Xe lamp, $\lambda \geq 285 \text{ nm}$	74.33	38	7
C <sub>3</sub> N <sub>4</sub> -rGO-WO <sub>3</sub>	1wt.% Pt	250W metal halide lamp, $\lambda \geq 420 \text{ nm}$	14.2	7.3	8
rGO-Co <sub>3</sub> (PO <sub>4</sub> ) <sub>2</sub>	None	300 W Xe lamp, $\lambda \geq 400 \text{ nm}$	6000	2970	9
Polymeric g-C <sub>3</sub> N <sub>4</sub> /rGO/Fe <sub>3</sub> O <sub>4</sub> composite	Pt	300 W Xe lamp, $\lambda \geq 400 \text{ nm}$	1157.5	530	10
N-doped defective graphene	RhCrO <sub>x</sub> /SrTiO <sub>3</sub> :Al	300 W Xe lamp,	6400	3016	11

**Table S4.** Composition of N-fGNS (determined from the full-range XPS spectrum) before and after 10 successive cycles of photocatalytic water splitting.

Samples	% of C	% of N	% of O
N-fGNS before photocatalytic water splitting	76.62	7.9	15.49
N-fGNS after 10 cycles of photocatalytic water splitting	77.15	8.12	14.56

## References

1. A. Jain, R. Balasubramanian and M. P. Srinivasan, *Chem. Eng.*, 2016, **283**, 789-805.
2. H. Ma, C. Li, M. Zhang, J.-D. Hong and G. Shi, *J. Mater. Chem. A*, 2017, **5**, 17040-17047.
3. L. Sun, L. Wang, C. Tian, T. Tan, Y. Xie, K. Shi, M. Li and H. Fu, *RSC Adv.*, 2012, **2**, 4498-4506.
4. D. Qu, M. Zheng, L. Zhang, H. Zhao, Z. Xie, X. Jing, R. E. Haddad, H. Fan and Z. Sun, *Sci. Rep.*, 2014, **4**, 5294.
5. H.-L. Guo, P. Su, X. Kang and S.-K. Ning, *J. Mater. Chem. A*, 2013, **1**, 2248-2255.
6. T. M. Suzuki, A. Iwase, H. Tanaka, S. Sato, A. Kudo and T. Morikawa, *J. Mater. Chem. A*, 2015, **3**, 13283-13290.
7. W.-N. Su, D. W. Ayele, H.-M. Chen, C.-J. Pan, V. Ochie, K.-T. Chiang, J. Rick and B. J. Hwang, *Mater. Today Energy.*, 2019, **12**, 208-214.
8. G. Zhao, X. Huang, F. Fina, G. Zhang and J. T. S. Irvine, *Catal. Sci. Technol.*, 2015, **5**, 3416-3422.
9. A. Samal, S. Swain, B. Satpati, D. P. Das and B. K. Mishra, *ChemSusChem*, 2016, **9**, 3150-3160.
10. Z. Pan, G. Zhang and X. Wang, *Angew. Chem.*, 2019, **131**, 7176-7180.
11. D. Mateo, A. García-Mulero, J. Albero and H. García, *Appl. Catal. B-Environ.*, 2019, **252**, 111-119.